PRINCIPAL COMPONENT ANALYSES FOR LITHOLOGIC AND ALTERATION MAPPINGS: Examples From The Red Sea Hills, Sudan

Nasir Hasen Kenea and Harald Haenisch
Freie Universität Berlin, Institute of Geology, Geophysics and Geoinformatics
Malteser str. 74-100, 12249 Berlin, Germany

Commission VII, Working Group 4

KEY WORDS: Mapping, Processing, Imagery, Landsat, GIS, Principal Component Analyses, Signal-to-Noise Ratio

ABSTRACT

Prinicipal Component Analyses (PCA) of Landsat-TM data covering parts of the Red Sea Hills, Sudan were conducted. Improved lithologic discrimination has been achieved, comapred to commonly used band composites like 7 4 1 and principal component images obtained from covariance matrix, through standardized transformation. The obtained image enhancement is corroborated by improved signal-to-noise ratio. Using feature-oriented PCA intended to enhance iron-rich and hydroxylated minerals, followed by low-pass filtering, it has been possible to successfully map alteration bodies related to sulphide and gold mineralisations. By computing band ratios and applying a GIS matrix-overlay technique substantial improvement has been achieved in mapping the alteration bodies enhanced through both processings. The latter appear less useful for lithologic mapping due to lack of morophological features and incorporation of noise.

1. INTRODUCTION

The Red Sea Hills (RSH) of the Sudan is an arid to semi-arid and rugged terrane with little or no vegetation cover. Geologically the region makes part of the Nubian Shield and is mainly covered by basement rocks that comprise of the older gneissic complexes, calc-alkaline metavolcano-sedimentary sequence of arc assembleges, migmatites and calc-alkaline granitoids, and mafic-ultramafic complexes related to ophiolitic suites (Vail, 1985). The tectono-thermal events that prevailed in the region are thought to be dominated by accretion tectonics of the Pan-African orogeny that gave rise to the development of prominant shear zones, complex fold patterns and related collisional structures. These geodynamical processes are thought to have also dictated the associated mineralizations (eg. Wipfler, 1994). In addition to the basement rocks there are isolated occurrances of younger sediments and Cenozoic volcanic rocks in a few localities over the RSH (Hassan, 1991).

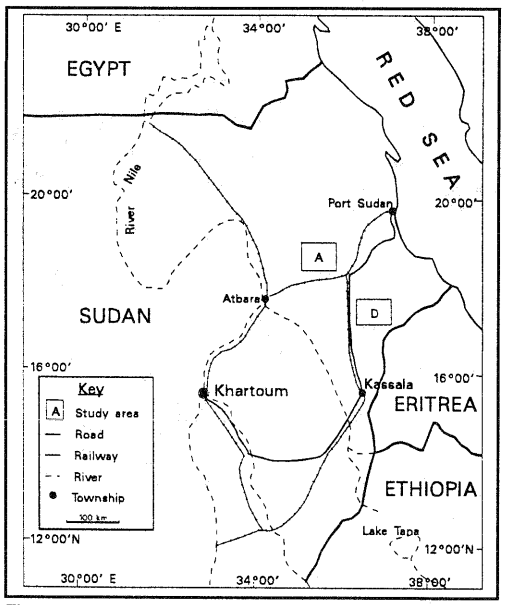

Figure 1. Location of the study areas; "D" for lithologic and "A" for alteration mappings.

As part of an on-going research on Landsat-data applications for geological studies, TM-imageries covering parts of the RSH (fig. 1) have been processed and interpreted. In this paper we present examples for which improved lithologic discrimination has been obtained and detection of alteration zones made possible using PC transformations.

2. LITHOLOGIC MAPPING

Part of a TM scene, path/row 171/48, captured on 06/10/1985 covering an area with diverse lithologies has been selected (area D, fig. 1) and geometrically corrected. Fast atmospheric correction was also applied following the method given by Chavez (1975). Commonly used band composites like 7 4 1 in R G B, respectively (Crippen, 1989) gave very impressive color, however, distinction among similar looking rocks such as rhyolite and dacite, metavolcano-sedimentary rocks with and without amphibole, graphitic schist and migmaitzed graphitic gneiss etc. appear difficult. PC transformation of the six reflective bands were conducted for the area of interest using covariance matrix (table 1), and individually analysed. As expected PC1, with 94.83% variance and positive loadings from all the TM bands, contains significant albedo and tpographic information. PCs 2, 3, and 4 mapped both morphological and spectral information pertaining to mineral composition in decreasing order, wheras PCs 5 & 6 are more of noise. Composites 1 2 3, and 1 2 4, in R G B, respectively, have been found to provide a better contrast. These composites, however, display no noticeable improvement over the row data composite in context of lithologic discrimination.

Standardized PC transformation (Singh & Harrison, 1985) was conducted for the study area using correlation coefficent (table 2) of the same input bands. Here the input bands are more or less uniformly weighted in the first PC, although the least correlated bands 1, 4 and 7 contribute relatively low. Bands 5 & 7 of the TM, that are dominant in the 1st PC in case of the unstandardized transformation (table 1) because of their larger variance, appear to contribute the highest in the 2nd PC for the standardized transformation. Examination of the variance distribution shows that in the latter case significant increament has been achieved for components 2,

a)

TM bands	1	2	3	4	5	7
1	135.14					
2	103.31	82.60				
3	176.27	141.66	248.62			
4	152.75	123.92	217.80	199.58		
5	268.44	217.98	386.27	346.35	692.95	
7	167.36	135.66	240.15	213.62	436.94	288.65

b)

	PC1	PC2	PC3	PC4	PC5	PC6
1	0.27	0.45	-0.59	-0.35	-0.44	-0.25
2	0.22	0.30	-0.15	-0.01	0.14	0.90
3	0.39	0.44	0.04	0.16	0.72	-0.34
4	0.35	0.34	0.59	0.39	-0.52	-0.01
5	0.66	-0.44	0.26	-0.55	0.03	0.02
7	0.42	-0.45	-0.47	0.63	-0.07	-0.01
Eigen v.	1562.29	62.14	12.13	6.76	3.34	0.87
Var. (%)	94.83	3.77	0.74	0.41	0.20	0.05

Table 1. Unstandardized PCA transformation; a) shows the covariance matrix and b) indicates the corresponding eigen matrices.

a)

TM-bands	1	2	3	4	5	7
1	1.00					
2	0.98	1.00				
3	0.96	0.99	1.00			
4	0.93	0.97	0.93	1.00		
5	0.88	0.91	0.93	0.93	1.00	
7	0.85	0.88	0.90	0.89	0.98	1.00

b)

	PC1	PC2	PC3	PC4	PC5	PC6
1	0.40	-0.44	-0.60	-0.47	-0.16	0.19
2	0.41	-0.32	-0.08	0.41	0.18	-0.72
3	0.42	-0.21	0.19	0.49	0.27	0.66
4	0.41	-0.13	0.71	-0.32	-0.45	-0.08
5	0.41	0.48	0.06	-0.43	0.64	-0.07
7	0.40	0.64	-0.30	0.30	-0.50	0.02

Table 2. Correlation coefficient (a) and the corresponding eigen matrix and variance (b) used for standardized PC transformation.

3, 5 and 6 (compare tables 1 & 2) making them much more informative. Consequently, study of the individaul PC images

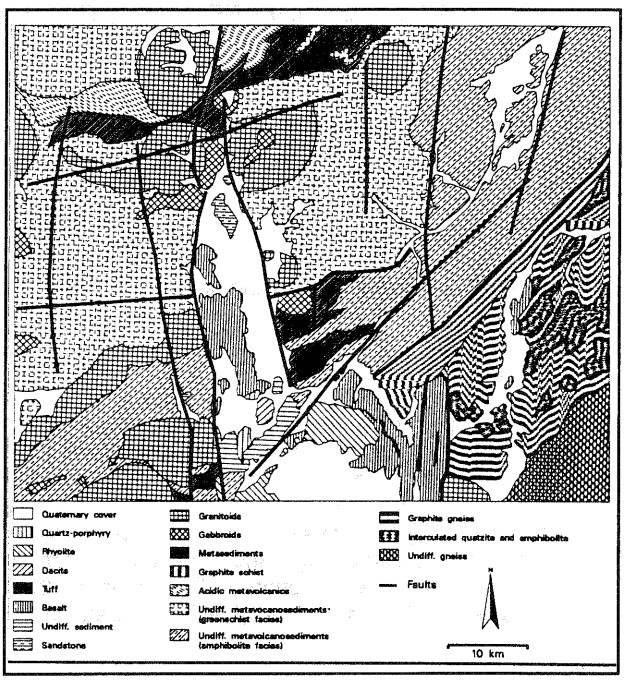

Figure 3. Geological interpretation map of the Odi sub-scene. Block-size is the same as fig. 2.

also revealed that PC2 (fig. 2, right) shows the best lithologic contrast and significant topographic information, followed by the 3rd and 5th components while the remaining PCs appear to be less informative in the present context. This gave bands 2 3 5 in R G B, respectively, as the composite with maximum spectral contrast.

On this composite similar looking rock units such as basalt and metasediments constituted by marble, metamorphosed siltstone, conglomerate, and graphitic schists etc. are well discriminable. Younger Phanerozoic sediments such as sandstone appear also distinct from undifferentiated sediments of mainly mudstone and conglomerates. Discrimination between rhyolite and dacite is well enhanced on this composite than on those from 7 4 1 of raw data or 1 2 3 composite from unstandardized PCA. Graphite rich rocks generally appear in bluish hue and well separable from the more acidic metavolcano-sedimentary sequence. The

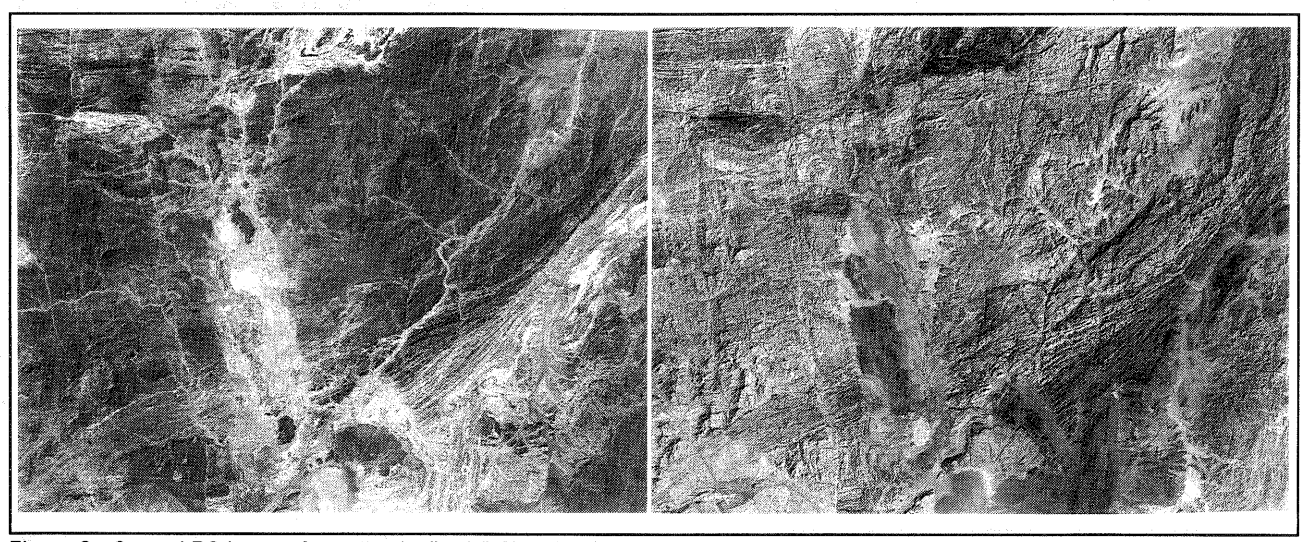

Figure 2. Second PC images for unstandardized (left) and standardized (right) transfomations. Note the spectral contrast and morphologic information contained in the latter. Block-size 77 km X 62 km.

obtained enhancement by using correlation coefficient instead of band covariance matrix is also supported by the improvement in signal-to-noise ratio. Following Ready & Wintz (1973) signal-to-noise ratio (SNR) may be determined as the ratio between the first eigen value and the maximum spectral band covariance. For the Ariab sub-scene;

using covariance matrix (table 1);

SNR = 1562.29/692.95 = 3.53 dB

whereas using correlation coefficient (table 2);

SNR = 5.65/1.0 = 7.52 dB

It can be seen that the obtained improvement is in the order of 3.99 dB, signifying the superiority of the standardized PC transformation. Furthermore, it should be noted that topographic expressions are well preserved in most of the PCs obtained from correlation coefficient and noise distribution is generally less, unlike the unstandardized components, facilitating more band combinations.

3. ALTERATION MAPPING

The Ariab Mininig District (AMD) of the central RSH is known for gold mineralisation associated with silica-barite lenses and dissiminated sulphides (Wipfler, 1994). These mineralisations are often surfacially represented by gossaniferous bodies of variable dimensions showing intense oxidation effects. Magnetite is the most abundant oxidation product observed in the massive sulphides (pyrite, sphalerite and chalcopyrite). The country rocks display effects of chloritization, sericitization, carbonisation, and silicification; whereas high flourine content & the formation of hydroxylated minerals added to the occurrance of alunite in the silica-barite suggest involvement of hydrothermal solutions (Wipfler, 1994). Figure 4 shows a generalized geological map of the Ariab area and the known gossaniferous bodies.

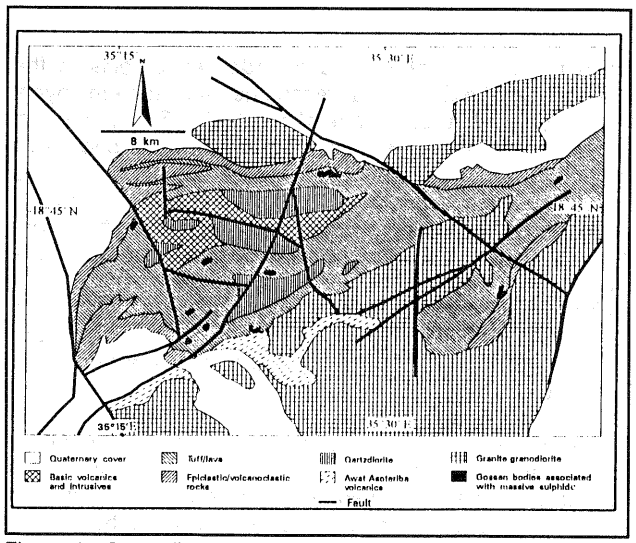

Figure 4. Generalized gological map of the Ariab area showing the major gossaniferous bodies (modified after Wipfler, 1994).

3.1 Feature Oriented PCA

The application of PC transformation for mapping alteration zones has been introduced through a technique called Feature Oriented PCA by Crosta & McM Moore (1989). In this approach four input bands, out of which the desired target has characterstic contrasting spectral features in two of them, are selected and processed. The eigen matrices contributed by these two bands are then examined for their significance in last two higher-order components. The desired target is often mapped in one of these PCs with opposite signs. Details of the method has been well elaborated in Loughlin (1991).

Two four-band sets: TM 1, 3, 4 & 7, and 1, 4, 5 & 7 covering the Ariab sub-scene (area "A", fig. 1) of the RSH (path/row 171/46) were selected to represent iron-oxide and hydroxyl-rich minerals, respectively. The data were then geocoded, atmospherically corrected and principal component transformations performed. The 1st PCs mapped albedo and topographic information whreas the 2nd PCs display the VIS/IR versus SWIR bands in contrasting signs as often the case is. The eigen vectors of PCs 3 & 4 were checked if they contain significant loadings in opposite signs from input bands of 1 & 3 and 5 & 7, as these band pairs are expected to display contrasting response for iron and hydroxyl-rich

a)

	TM1	TM3	TM4	TM7
PC1	0.38	0.60	0.53	0.46
PC2	-0.07	-0.24	-0.43	0.87
PC3	-0.84	-0.06	0.52	0.18
PC4	0.39	-0.76	0.51	0.08

b)

	TM1	TM4	TM5	TM7
PC1	0.33	0.46	0.71	0.42
PC2	-0.30	-0.69	0.22	0.62
PC3	0.84	-0.25	-0.39	0.27
PC4	-0.30	0.50	-0.55	0.60

Table 3. Eigen vector loadings of the Ariab sub-scene; a) for "iron-oxide" mapping using bands 1, 3, 5 and 7, b)for "hydroxyl" mapping using TM bands 1, 4, 5 and 7.

minerals, respectively (Loughlin, 1991). In both of the considered cases PC4 appears to have mapped the iron-oxide (-0.76) and hydroxyl-rich (-0.55) minerals in dark pixels (table 3), and to obtain them as bright pixels these images have been negated. This operation excludes the effect of vegetation from both PCs by mapping them in dark pixels.

The next important step was to filter the images by 3X3 low-pass matrix in order to supress the obviously incorporated high noise. The effect of noise is apparently well pronounced in the "hydroxyl" image possibly due to band-5 that also has the largest variance and overall reflectance. A "mixture" image was also produced by linear combination of the two images. A composite image has been finally obtained by using the "hydroxyl", "mixed" and "iron-oxide" imges in R, G and B, respectively. Figure 5 shows the "iron-oxide" and "hydroxyl" images before and after fileting.

Comparison of the the obtained composite with available map (Wipfler, 1994) has shown that all the known mineralisations have been mapped in a distinct yellowish color against the bluish-red country rocks (Kenea, 1996). It is also possible to suggest other potential sites which may require field verificastions. Furthermore, it is to be interpreted that the yellowish hue suggests the dominance of hydroxylated-silicates in the mineralisation, and could be followed also along most slopes close to the insitu altered rocks.

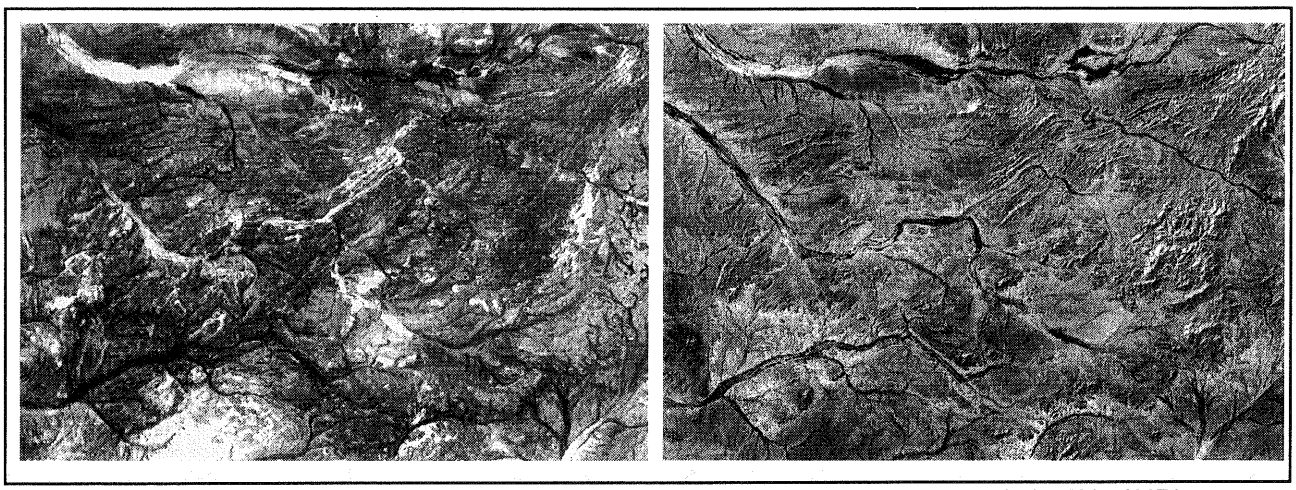

Figure 5. "hydroxyl" (left) and "iron-oxide" (right) images of the Ariab sub-scene before filtering. Block-size 53 km X 37 km.

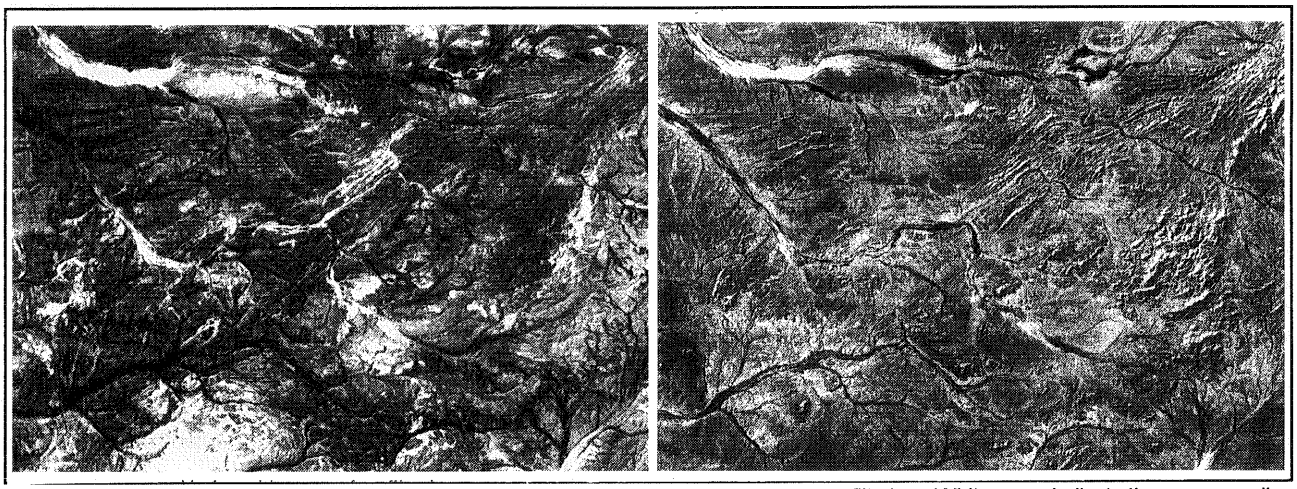

Figure 6. "Hydroxyl" (left) and "iron-oxide" (right) images of the Ariab sub-scene after low-pass filtering. White areas indicate the corresponding potential mineralisations. Block-size is the same as in figure 5.

3.2 GIS Overlay

Close observation of the above composite also revealed that Recent unconsolidated sediments along river channels partly exhibit a signature similar to the gossan bodies. In order to avoid the coroboration of such undesired objects in the "alteration map" a GIS overlay technique has been employed. In this approach a ratio image of bands 5/7, 5/4, and 3/1 (in R, G, B, respectively) was initially computed and checked if the altered rocks could be discriminated. On this composite image the gossan bodies show a yellowish-green color in contrast to the country rocks and are also well distinct from the sediments, however not all the known mineralisations are mapped in the latter (Kenea, 1996). The GIS matrix-overlay technique is thus conducted in order to combine the information from these two alteration mapping methods and produce a map containig only alteration bodies related to the mineralisations.

Cl.	1	2	3	4	5	6	7	8
1	17.6	8.6	4.1	13.1	0.4	0.9	1.0	0.1
2	44.0	66.3	4.0	33.6	0.0	9.0	10.0	0.0
3	8.2	1.2	60.9	6.1	3.5	4.7	17.2	0.0
4	8.2	6.2	4.4	16.0	1.1	3.6	4.9	0.4
5	1.0	0.0	4.1	1.5	90.2	0.5	2.4	0.2
6	10.4	9.4	14.7	15.8	2.4	71.2	34.1	0.0
7	10.6	8.4	7.8	13.9	2.4	10.2	30.3	0.0
8	0.0	0.0	0.0	0.0	0.0	0.0	0.0	99.5

Table 4. Error matrix of the training classes used for the classification of the Feature-oriented PC image. The columns show the classified data whereas the rows indicate the reference data. Values are in percentage, rounded to the nearest decimal. Classes 1 to 8 refer to Awat-vol., basic intrusives and volcanics, epiclastic rocks, granodiorite, gossan, quartzdiorite, tuff/lava and Quaternary sediments, respectively (fig. 4).

The above obtained two color composite images were then separately classified into 8 classes using supervied classificsation method based on a priori knowledge obtained from available map (figure 4). The separability of the training areas appears generally good and the computed error matrix shows negligible misclassification between the gossans and the unconsolidated sediments (table 4). This gave two GIS files with 8 classes each. The obtained classified files were then examined and it has been found out that the sediments and the gossans have been mapped separately and the mixture of pixels between the two is in the order of 28% for the Feature-oriented PCA and 15% for the ratio images.

The next step was to recode the different classes using an off-set of 1, the alteration bodies were recoded as 1 whereas all the remaining classes as 0. The obtained two recoded files were then joined using a matrix overlay technique with an "intersection" function, whereby those pixels having a value of 0 and 0, 0 and 1, or 1 and 0 in the GIS files obtained form band-ratioing and Feature-oriented PC transformation, respectively were regrouped accordingly as classes 1, 2, and 3 whereby they were given a new value of 0. Those pixels having a value of 1 in both GIS files, and thus correspond to the alteration bodies, were grouped as class 4 and obtained a new value of 1. Further rifining was carried out to omit isolated random pixels or group of pixels less than about 100mX100m size by runing a 3X3 low-pass filter. The resulting binary image appears to have succeeded in excluding the undesired Quaternary sediments and has substantially mapped the gossaniferous bodies (Kenea, 1996). Interestingly the image has also managed to exclude basic metavolcanics that did exhibit a similar feature as the altered rocks on the ratio image produced by List, et. al. (1992, personal comm.) for the same area.

4. CONCLUSION

The applied standardized PC transformation has proven useful for lithologic discrimination among rocks with subtle chemical difference where commonly used band composites failed to give good results. Furthermore, in addition to data compression, it provided images with higher signal-to-noise ratio that allowed more band combinations thereby enabling improved mapping of the rock units in the area. Known hydrothermally altered areas and gossaniferous bodies have been successfully mapped by using Feature-oriented PCA followed by low-pass filtering, making the method recommendable for exploration in similar occurrances. Computation of band-ratio composites followed by a GIS matrix-overlay technique have substantially improved the result by excluding undesired objects. The latter operations appear least useful for lithologic discrimination, mainly for lack of morphological features useful for geologic image interpretation, longer processing steps and involvement of noise.

5. ACKNOWLEDGEMENTS

Field works were conducted under the Special Research Project-69 (SFB-69), sub-project F5/E7, financed by the Deutsche Forschungsgemeinschaft (German Research Foundation). The stay of the first author in Germany was sponsored by the German Academic Exchange Service (DAAD). The research has been supervised by Prof. F. K. List. All colleagues at the remote sensing section (FU) are thanked for their assistance at several stages of the work, particularly R. Schöler for keeping the computers running.

6. REFERENCES

Chavez, P. S., 1975, Atmoshpheric, solar & MTF correction for ERTS digital imagery. In: Proceedings of American Society of Photogrammetry meeting in Phoenix, Falls Church, Virginia (U.S.A.), (Falls Church, VA: American Society of Photogrammetry), pp. 69-69a.

Crippen, R. E., 1989, Selection of Landsat TM band and band-ratio combinations to maximize lithologic information in color composite displays. Proceedings of the 7th Thematic Conference: Remote Sensing for Exploration Geology, Calgary, Alberta, Canada, Oct. 2-6, pp. 917-921.

Crosta, A. P., and McM. Moore, J., 1989, Enhancement of Landsat thematic mapper imagery for residual soil mapping in SW Minas Gerais State, Brazil: A prospective case history in greenstone belt terrane. Proceedings of the 7th Thematic Conference: Remote Sensing for Exploration Geology, Calgary, Alberta, Canada, Oct. 2-6, pp. 1173-1187.

Hassan, A. S., 1991, Cenozoic volcanic rocks and intraformational sediments from the Red Sea Hills, Sudan. Unpubl. M.Phil. Thesis, Portsmouth Polytechnic, U. K.

Kenea, N. H., 1996, Digital image processing and GIS data integration for geological studies in the Southern Red Sea Hills, Sudan. PhD. Thesis (in prep.), Freie Universitäat Berlin, Germany.

List, F. K., Koch, W., and Salahchourian, M. H., 1992, Geological mapping in arid regions of Africa using sattelite data-intergration of visual and digital techniques. In: International Archives of Photogrammetry and Remote Sensing, Washington DC, USA, vol. XXIX, Part B4, pp. 325-332.

Loughlin, W. P., 1991, Principal component analyses for alteration mapping. Photogrammetric Engineering and Remote Sensing, 57 (9), 1163-1169.

Singh, A., and Harrison, A., 1985, Standardized principal components. International Journal of Remote Sensing, Vol. 6, No. 6, pp. 883-896.

Vail, J. R., 1985, Pan-African (Late Precambrian) tectonic terranes and the reconstruction of the Arabian-Nubian Shield. Geology, 13: 839-842.

Wipfler, E., 1994, Geochemishce, strukturelle und erzmikroskopische Untersuchungen zur Lagestaätten-entwicklung des Ariab Nakasib Belt, Red Sea Provinz, NE Sudan. Berl. Geow. Abh., A, pp.206, Berlin (Selbstverl. FB Geow., FU Berlin).